Chapter 1. Introduction

Research over the past four decades has revealed that cancers are caused by mutations which favor cellular dysregulation, proliferation, and further mutation. Mutated protein kinases play a major role in the disease process. Normally, these kinases are central to cellular regulation by signal transduction, the transfer of a signal from the cell membrane to the nucleus, and also cell-cycle control and cell division. Protein kinases catalyze the transfer of the terminal phosphate group from adenosine triphosphate (ATP) to the hydroxyl group of a serine, threonine, or tyrosine residue of the kinase itself, another kinase or another protein substrate (Fig. 1). These kinases may adopt a number of conformations which may be active (i.e., on the catalytic pathway) or inactive.[1]

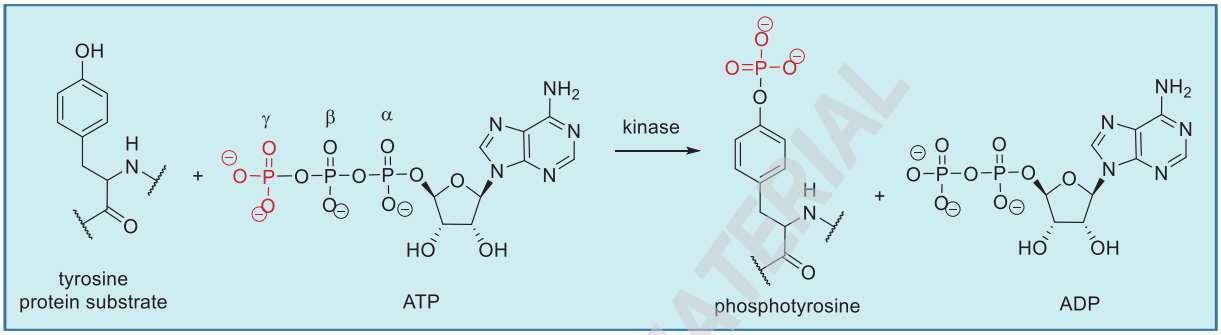

Figure 1. Protein kinase-catalyzed transfer of a γ-phosphoryl group from ATP onto target tyrosine side chain of a protein substrate.

COPYRIGHTED MATERIAL

1.1 Types of Protein Kinases[2]

The human kinome contains 518 known protein kinases: 478 typical and 40 atypical kinases. According to the sequence similarity of their kinase domains, typical kinases are divided into eight groups: TK (tyrosine kinase, 90), TKL (tyrosine kinase-like kinase, 43), STE (STE7-, STE11-, and STE20-related kinase, 47), CK1 (casein kinase 1, 12), AGC (protein kinase A/G/C-related kinase, 63), CAMK (Ca2+/calmodulin-dependent kinase, 74), CMGC (CDK/MAPK/GSK/CDK like-related, 61), and RGC (receptor guanylyl cyclase, 5). The 40 atypical protein kinases include PI3K (lipid kinase) and mTOR (serine/threonine protein kinase).

TKs are further classified as RTKs receptor tyrosine kinases (RTKs) and non-RTKs. RTKs are transmembrane proteins with an extracellular and intracellular kinase domain. They become activated upon dimerization, triggered by the binding of their ligands to the extracellular domain. RTKs have been extensively exploited as anticancer therapeutics, for example, EGFR/HER family proteins, VEGFR, TRK, ALK, ROS1, FLT3, PDGFRs, and FGFRs. Non-RTKs include SRC, ABL, and JAK.

The TKL family consists of serine/threonine kinases, with sequences similar to those of the TK group, including IRAK, BRAF, LIMK, and TGFβ. Three families of STE kinases have been found: STE20 (MAP4K), STE11 (MAP3K), and STE7 (MEK), while CDKs, MAPK, GSK, and CDK-like kinases constitute the CMGC group.

1.2 Protein Kinase Domains

The 518 human protein kinases share a number of common features (depicted in Fig. 2), including (1) separate N- and C-terminal lobes (domains) connected by an intervening peptide chain (linker or hinge region) which also provides a binding site for the universal phosphoryl donor ATP; (2) availability of an active conformation which can bind ATP and accelerate phosphorylation of the specific protein which is downstream on the signaling pathway; and (3) a conserved sequence of aspartate (D), phenylalanine (F), and glycine (G) in the ATP-

Molecules Engineered Against Oncogenic Proteins and Cancer, First Edition. E. J. Corey and Yong-Jin Wu.
© 2024 John Wiley & Sons Inc. Published 2024 by John Wiley & Sons Inc.

binding region of the linker (DFG motif) located on the N-terminal side of the activation loop. Many kinases can also adopt other conformations which do not bind ATP or catalyze phosphorylation of the downstream protein.

The structure of BCR-ABL kinase is depicted in Figure 2 which shows the relative locations of the various subregions. It is typical of the large family of kinases. Conformational transitions between kinase states are orchestrated by the movement of five conserved structural motifs in the catalytic domain: (1) the αC helix (helix in, active; helix out, inactive); (2) the DFG motif (DFG-Asp-in, active; DFG-Asp-out, inactive) which forms part of the ATP-binding site in the kinase; (3) the activation loop (A-loop open, active; A-loop closed, inactive); (4) the ATP-binding of glycine-rich loop (P-loop binding, active conformation; P-loop nonbinding, inactive); and (5) the hinge region (linker region), which varies in location between the N-terminal domain (N-lobe) and the C-terminal domain (C-lobe).[3]

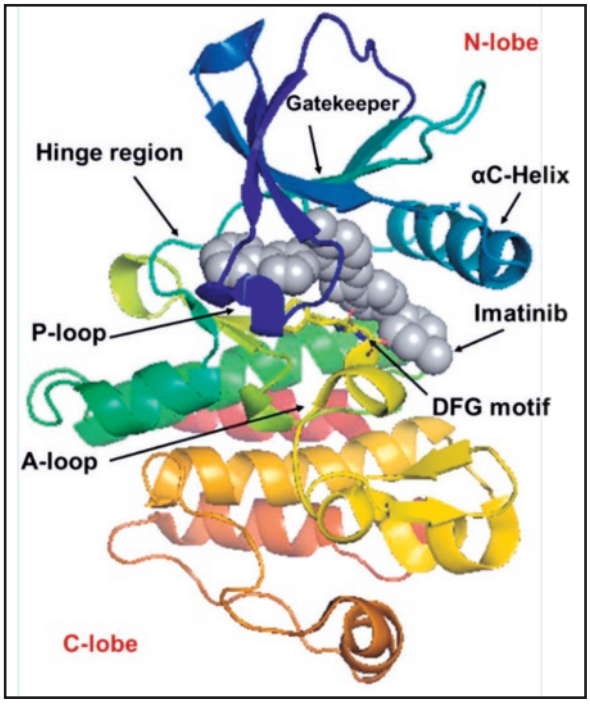

Figure 2. X-ray crystal structure of BCR-ABL with imatinib bound and with key structural motifs highlighted. Adapted from PDB: 2HYY.

One hallmark of an active conformation is that the aspartate of the DFG motif points toward the ATP-binding site (DFG-Asp-in, or DFG-in for simplicity) and coordinates two Mg^{2+} ions. Another hallmark is that the αC helix located on the N-terminal domain is rotated inward toward the active site (αC-in). A different and inactive conformation involves a translocation of the positions of the Asp and Phe residues, which moves the aspartate away from the ATP-binding site by ~5 Å to generate a catalytically incompetent state, the DFG-Asp-out (or DFG-out) state. The resulting conformation has a new allosteric pocket adjacent to the ATP-binding pocket which can be exploited by type II inhibitors to gain selectivity.

1.3 ATP-Binding Site[4–7]

ATP binds to a narrow hydrophobic pocket located between two lobes connected by a flexible hinge region containing three conserved residues (Fig. 4). These hinge residues, which form part of the ATP-binding pocket, engage several key H-bonds with the heteroaromatic adenine ring of ATP (Fig. 3). The hinge region is the primary target of most ATP-competitive kinase inhibitors possessing a hinge-binding motif. These inhibitors are designed to form some or all of the same key hydrogen-bonding acceptor and donor interactions with the hinge backbone atoms as adenine of ATP, thereby competitively displacing ATP from the binding site.

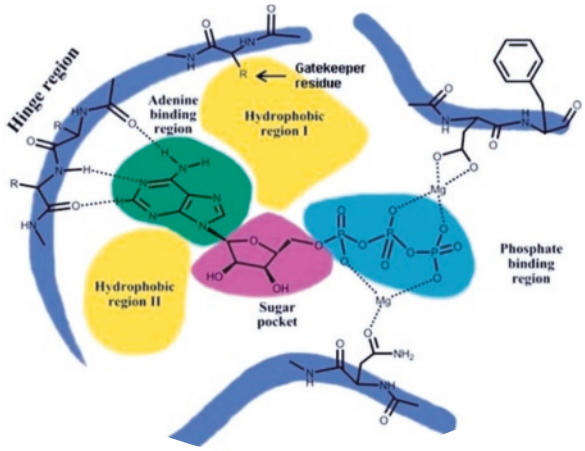

Figure 3. ATP-binding site of a typical protein kinase. Adapted from *ACS Chem. Biol.* **2013**, *8*, 1044–1052.

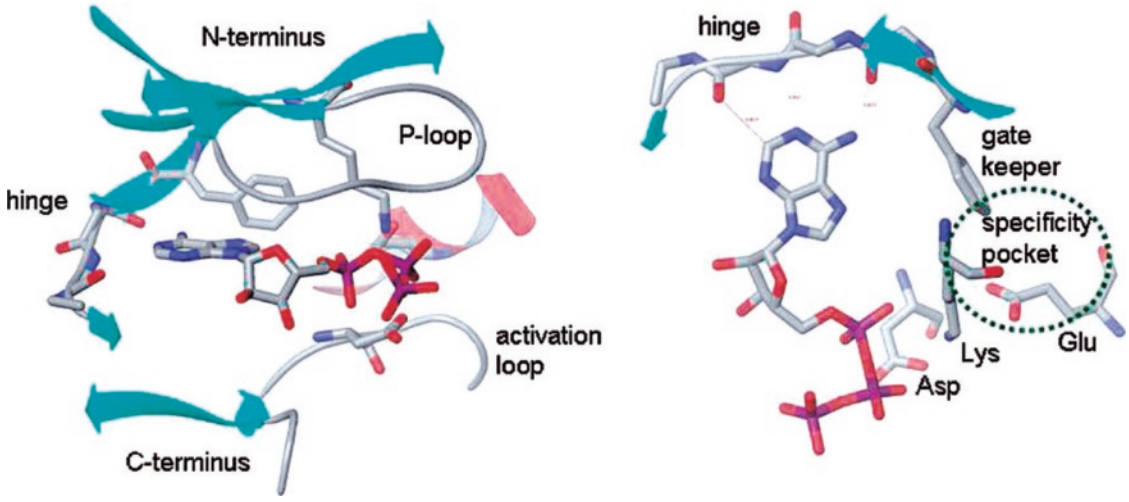

Figure 4. ATP-binding site. Left: ATP binds between the N- and C-termini. The P-loop forms the roof, and a C-terminal β-sheet covers the floor. Right: Gatekeeper and conserved lysine, glutamate (of αC-helix), and Asp of the DFG motif control access to specificity pocket. Adapted with permission from *J. Med. Chem*. **2008**, *51*, 5149–5171.

Determinants of the selectivity in kinases include the conformation of the DFG motif at the start of the A-loop and the conformation of the P-loop.[8] Both DFG-Asp-out and DFG-Asp-in conformations have been observed in binding with various selective kinases (Fig. 5). The P-loop can contribute to this selectivity by forming extensive contacts with the inhibitor.

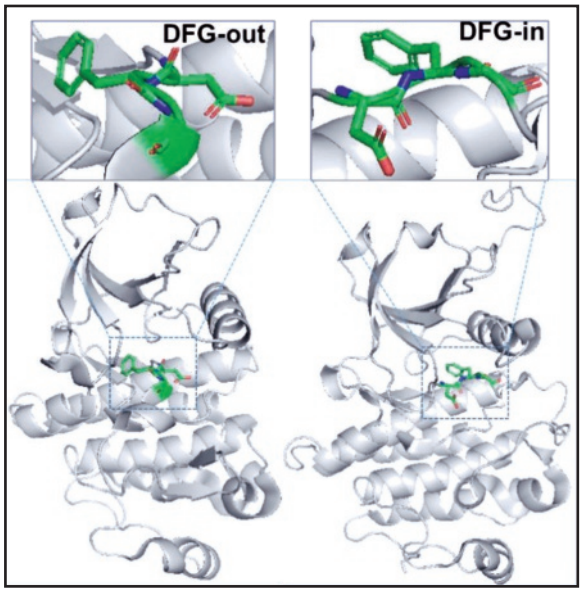

Figure 5. The DFG-Asp-out or DFG-Asp-in conformations in ABL (PDB ID: 2HYY and 2GQG).

Kinase domains contain a gatekeeper residue, located at the beginning of the hinge region. It is the single most important residue in the ATP-binding site, which partially or fully blocks a hydrophobic region deep in the ATP-binding pocket, depending on the size/volume of the gatekeeper's side chain. The gatekeeper residue also contributes to the selectivity for small-molecule kinase inhibitors.

1.4 Types of Kinase Inhibitors[9–16]

In general, there are two types of kinase inhibitors: covalent and non-covalent inhibitors. The latter can be divided into four major classes according to their binding mode.

Type I inhibitors (such as dasatinib, Figs. 6, 7, 10) bind to the DFG-in, αC-in active conformation of the kinase with the Asp of the DFG motif pointing into the ATP-binding pocket. Type 1 inhibitors take advantage of the gatekeeper residue for selectivity. The majority of FDA-approved kinase inhibitors are type I inhibitors, e.g., gefitinib, erlotinib and sunitinib.

Type II inhibitors (such as imatinib, Figs. 6, 7, 10) bind to the DFG-out, αC-out inactive conformation with the Phe of the DFG motif pointing into the ATP-binding pocket. In the DFG-out conformation, Phe and Asp have switched positions relative to the DFG-in conformation, resulting in the opening of a new hydrophobic allosteric pocket adjacent to the ATP site. The additional binding to this allosteric pocket enhances the selectivity of type

II inhibitors as compared with type I. The type II class includes nilotinib and sorafenib.

Type I1/2 is between type I and type II. The EGFR inhibitor lapatinib falls into this class which binds to a DFG-in, αC-out inactive conformation (Figs. 8, 9). In this case, the EGFR adopts a DFG-in conformation, typical of an active kinase; however, the αC helix is pushed out (αC-out) by the fluorobenzyl substituent of the inhibitor, resulting in the disruption of the ion pairing between the active site Lys and the Glu from the αC helix and an inactive conformation. As a result, the fluoro-benzyl substituent extends into an allosteric pocket opened by the outward, inactive position of the αC helix. Vemurafenib is another type I1/2 inhibitor that binds to a DFG-in, αC-out inactive conformation of BRAF.

Type III inhibitors bind to an allosteric pocket next to the ATP-binding pocket (Fig. 10), with no hydrogen bond interactions with the hinge residues. They induce conformational changes in the activation loop, forcing the αC helix to adopt an inactive conformation. The type III class includes MEK inhibitors such as trametinib and binimetinib.

Type IV inhibitors bind to any allosteric sites distant from the ATP-binding pocket (Fig. 10). They induce conformational changes to lock the protein into an inactive state. For example, asciminib is a type IV allosteric inhibitor of BCR-ABL that binds to a myristoyl site of the BCR-ABL protein.

Covalent kinase inhibitors (CKIs) usually target an active site cysteine in or around the ATP-binding site. Covalent inhibition is typically irreversible, but can be reversible, depending on the nature of the electrophilic warhead. CKIs have been developed for various protein kinases, including FGFR, VEGFR-2 and BTK. Covalent, irreversible KRAS(G12C) inhibitors have recently been brought to market.

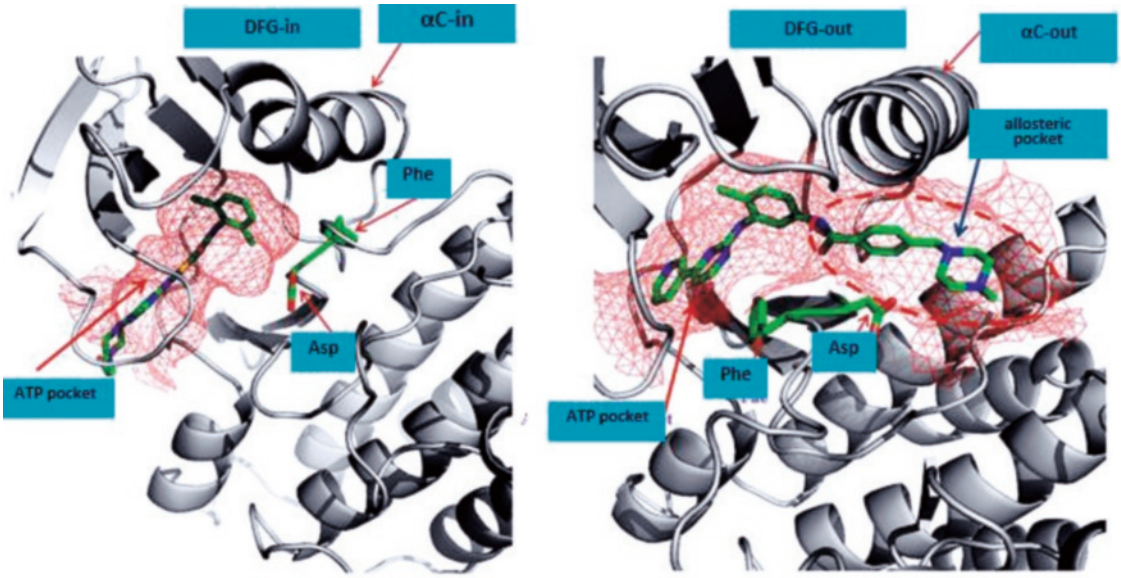

Figure 6. Type I vs. type II inhibitors. Adapted with permission from *J. Med. Chem.* **2015**, *58*, 466–479.

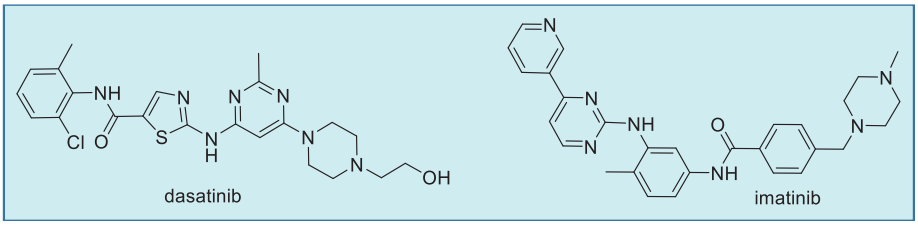

Figure 7. Structures of dasatinib and imatinib.

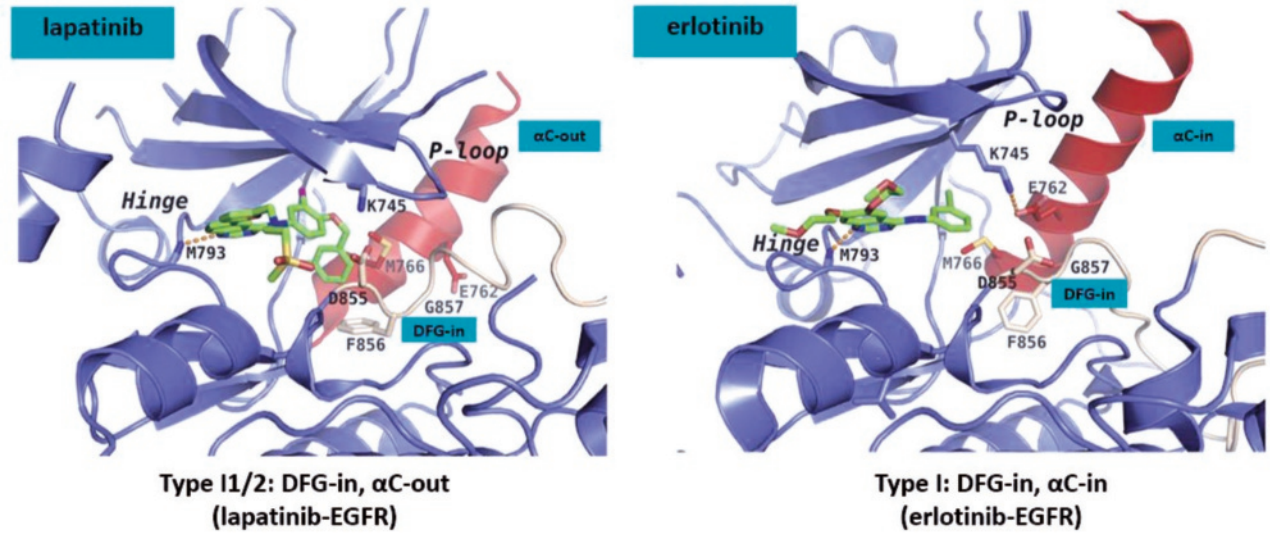

Figure 8. Type I1/2 vs. type I inhibitors. Adapted from *J. Biol. Chem.* **2011***, 286*, 18756–18765.

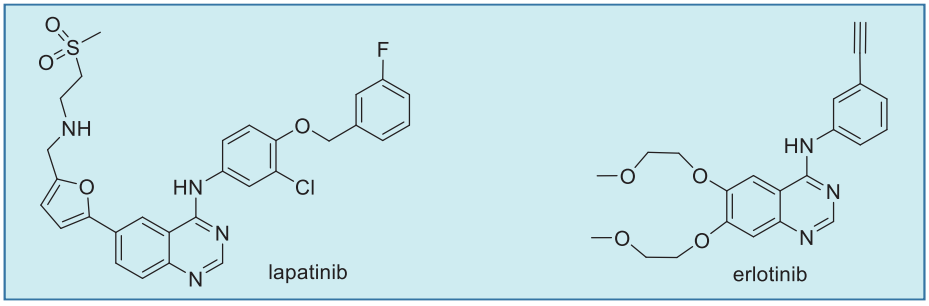

Figure 9. Structures of lapatinib and erlotinib.

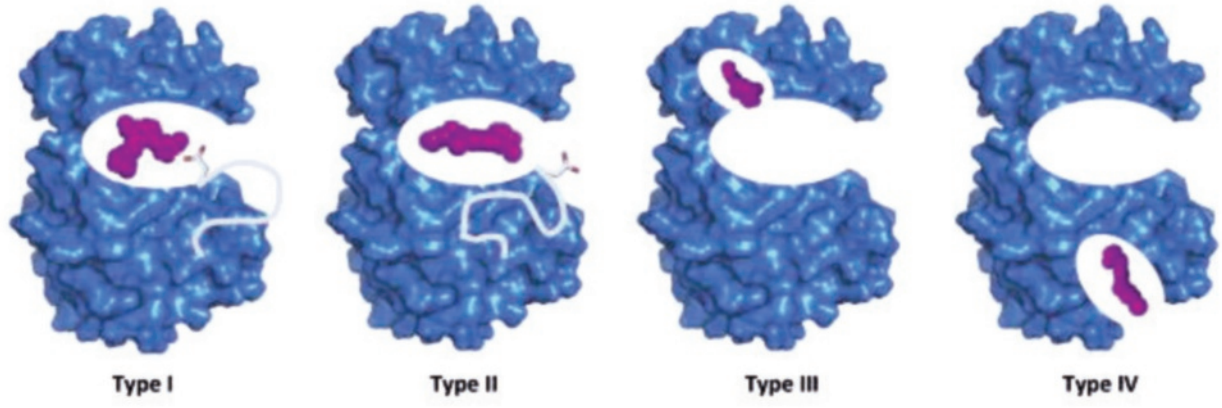

Figure 10. Cartoon illustration of 4 types of inhibitors. Type I: DFG-in active conformation; Type II: DFG-out inactive conformation; Type III: allosteric pocket close to ATP-binding site; Type IV: allosteric pocket remote from the ATP site. Adapted from *Trends Pharmacol. Sci.* **2015**, *36*, 422–439.

1.5 Brief History of Small-molecule Kinase Inhibitors

In 1981, a screening project with a variety of natural products for antitumor activity by the U.S. National Cancer Institute (NCI) identified rapamycin (Fig. 11) as a unique anticancer agent. Against the 60 tumor cell line panel, rapamycin potently inhibited the growth of a number of solid tumors, a significant

finding at the time because it was the very first non-toxic cytostatic agent. Approximately 20 years after the discovery of its antitumor activity, it was determined that the target of rapamycin is the protein mTOR. Binding of rapamycin to mTOR blocks the PI3K/AKT/mTOR signal transduction pathway, and the complete structure of mTORC1 was elucidated in 2005. Rapamycin was approved by the FDA in 1999 as an immunosuppressant drug.

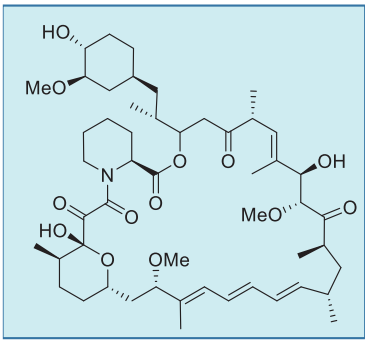

Figure 11. Structure of rapamycin.

Staurosporine (Fig. 12), a basic polycyclic natural product first isolated in 1977, did not attract significant attention until 1986 when it was shown to be the first broad spectrum protein kinase inhibitor. Staurosporine itself is too toxic to be used as a drug. Subsequent medicinal chemistry efforts led to the *N*-benzoyl derivative, later known as midostaurin, which displayed improved selectivity. Because of its broad kinase inhibition profile and its efficacy to shrink tumors in murine tumor xenograft models, midostaurin entered into clinical trials in 1991 – four years ahead of imatinib (in 1995) – for the treatment of solid tumors. However, its potent antitumor activity did not translate into clinical efficacy. Unfortunately, there was no biomarker at the time to monitor its target proteins and it was difficult to predict who might benefit from the drug. In 2001, midostaurin was identified as a potent FLT3 tyrosine kinase inhibitor by a collaborative effort between the Dana-Farber Cancer Institute and Novartis to discover inhibitors of mutant FLT3-positive AML in cellular assays. It was this finding that led to the repurposing of a twice failed drug for FLT3 mutant AML. Midostaurin was approved by the FDA in 2017 for newly diagnosed FLT3-mutated AML.

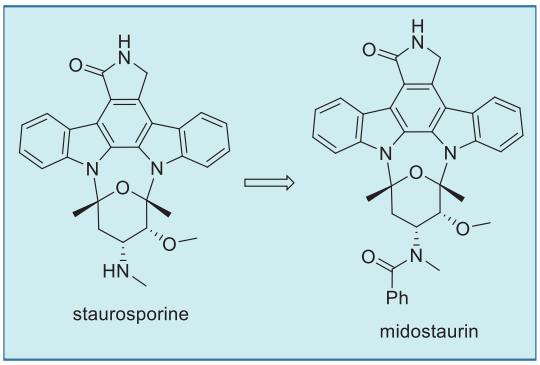

Figure 12. From staurosporine to midostaurin.

The modern era of protein kinase drug discovery was initiated in 1988 at Ciba-Geigy by biochemist Nick Lydon in collaboration with Brian Druker of Oregon Health and Science University (OHSU) as an effort to develop targeted chemotherapies for CML. At the time, most pharmaceutical companies believed that selective inhibition of a specific tyrosine kinase among >500 was unlikely because of their similarity and the likelihood of adverse off-target side effects. Despite such skepticism of the feasibility of developing selective kinase inhibitors, the joint effort was successful and ultimately led to the antileukemic BCR-ABL oncoprotein inhibitor imatinib (Fig. 13) as a preclinical candidate in 1995. The discovery of imatinib ushered in the era of kinase inhibitors as targeted therapies.

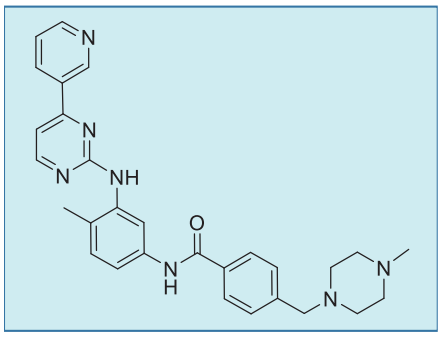

Figure 13. Structure of imatinib.

In 1991 – three years after Ciba-Geigy started the CML program, Sugen was founded with the mission of developing selective protein kinase

inhibitors. Scientists at Sugen were seeking small-molecule VEGFR inhibitors to block the VEGF/VEGFR signaling pathway and subsequently attenuate blood vessel formation required for tumor growth, while Genentech was focusing on monoclonal antibodies that bind to VEGFs to prevent activation of their receptors VEGFRs. Sugen's early multikinase inhibitors that cross-inhibit VEGFRs were disappointing in clinical trials due to poor PK, but subsequent optimizations led to sunitinib (Fig. 14), which was approved in 2006 for gastrointestinal stromal tumor (GIST) and renal cell carcinoma (RCC), following only one month after Bayer's sorafenib (Fig. 14) which was initially identified as a RAF inhibitor and subsequently shown also to inhibit several VEGFRs.

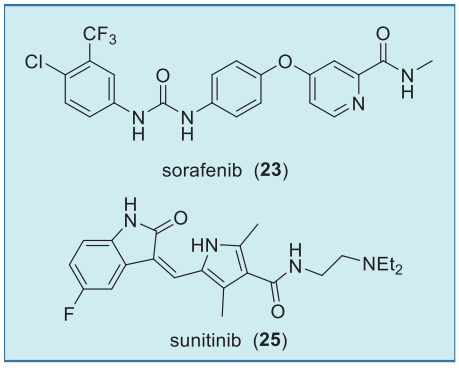

Figure 14. Structures of sorafenib and sunitinib.

1.6 Peak 12-Month Sales for Leading Kinase Inhibitors

1. Ibrutinib (BTK): $9.7 billion (2021)
2. Palbociclib (CDK4/6): $6.0 billion (2022)
3. Osimertinib (EGFR): $5.4 billion (2022)
4. Imatinib (BCR-ABL): $4.7 billion (2016)
5. Ruxolitinib (JAK1/2): $3.97 billion (2022)
6. Nintedanib (PDGFR/VEGFR/FGFR): 3.6 billion (2022)
7. Tofacitinib (pan-JAK): $2.5 billion (2020/21)
7. Abemaciclib (CDK4/6): $2.5 billion (2022)
9. Dasatinib (BCR-ABL): $2.1 billion (2019)
9. Nilotinib (BCR-ABL): $2.1 billion (2021)
9. Everolimus (mTOR): $2.1 billion (2021)
9. Acalabrutinib (BTK): $2.1 billion (2022)
13. Cabozantinib (RET): $1.9 billion (2022)
14. Upadacitinib (JAK1): $1.8 billion (2022)
15. Erlotinib (EGFR): $1.5 billion (2014)
15. Alectinib (ALK): $1.5 billion (2022)
17. Sunitinib (VEGFR): $1.2 billion (2014)
17. Ribociclib (CDK4/6): $1.2 billion (2022)
19. Sorafenib (VEGFR): $1 billion (2014)
20. Dabrafenib (BRAF)/trametinib (MEK): $0.9 billion each (2022)

1.7 Approved Kinase Inhibitors

As of January 01, 2023, there are 78 FDA-approved small-molecule kinase inhibitors (Figs. 15-34) and two KRAS(G12C) inhibitors (Fig. 35) (also see Appendix 1: First FDA Approvals by Year) for the treatment of a variety of diseases, especially cancer. All these inhibitors are oral medications except for netarsudil, which is available as an ophthalmic solution (eye drops), and temsirolimus, copanlisib, and trilaciclib that are administered intravenously.

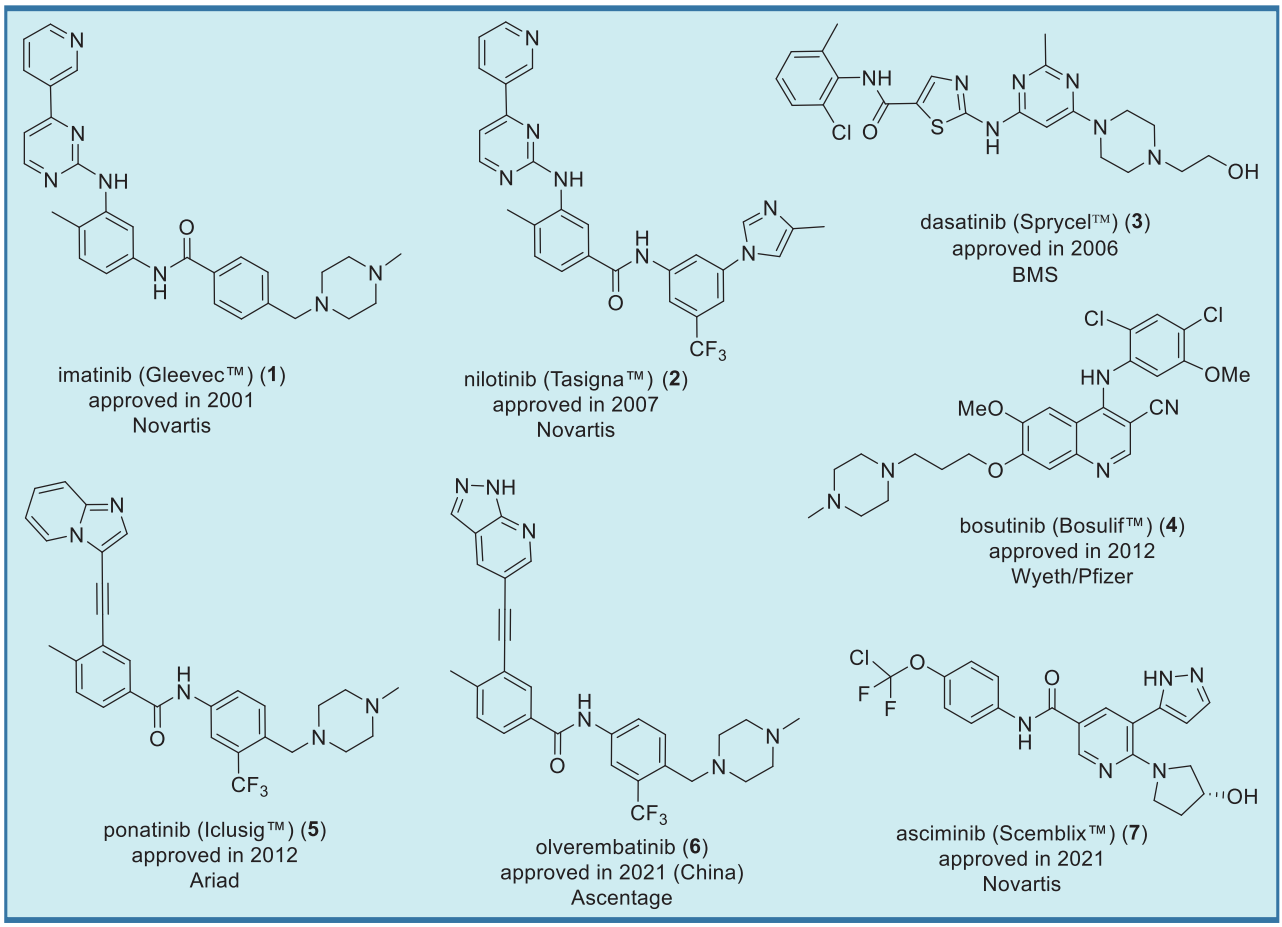

Figure 15: BCR-ABL inhibitors (Chapter 2).

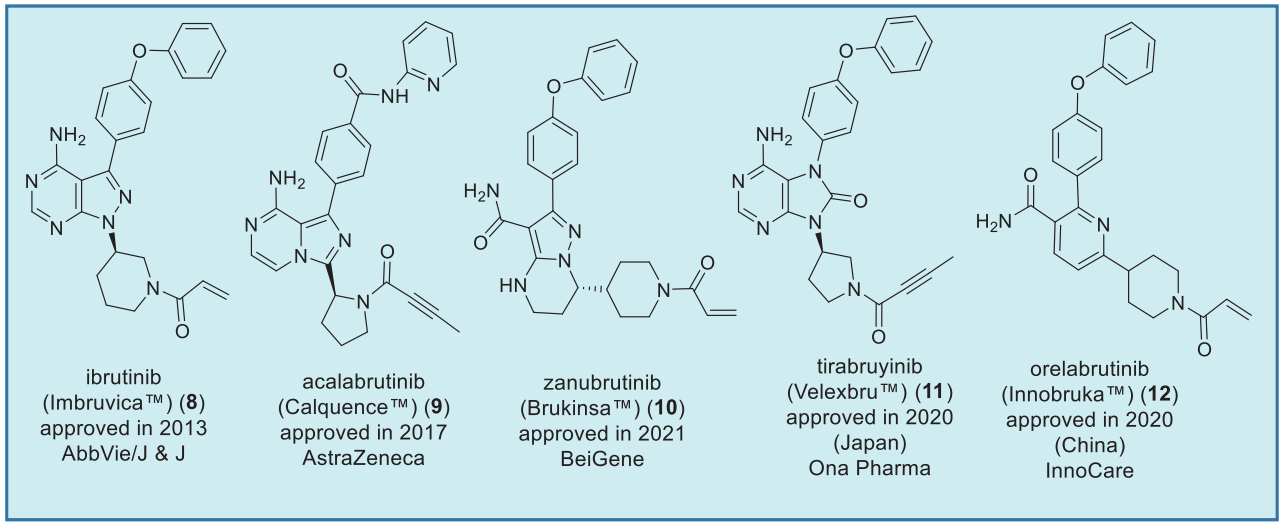

Figure 16. BTK inhibitors (Chapter 3).

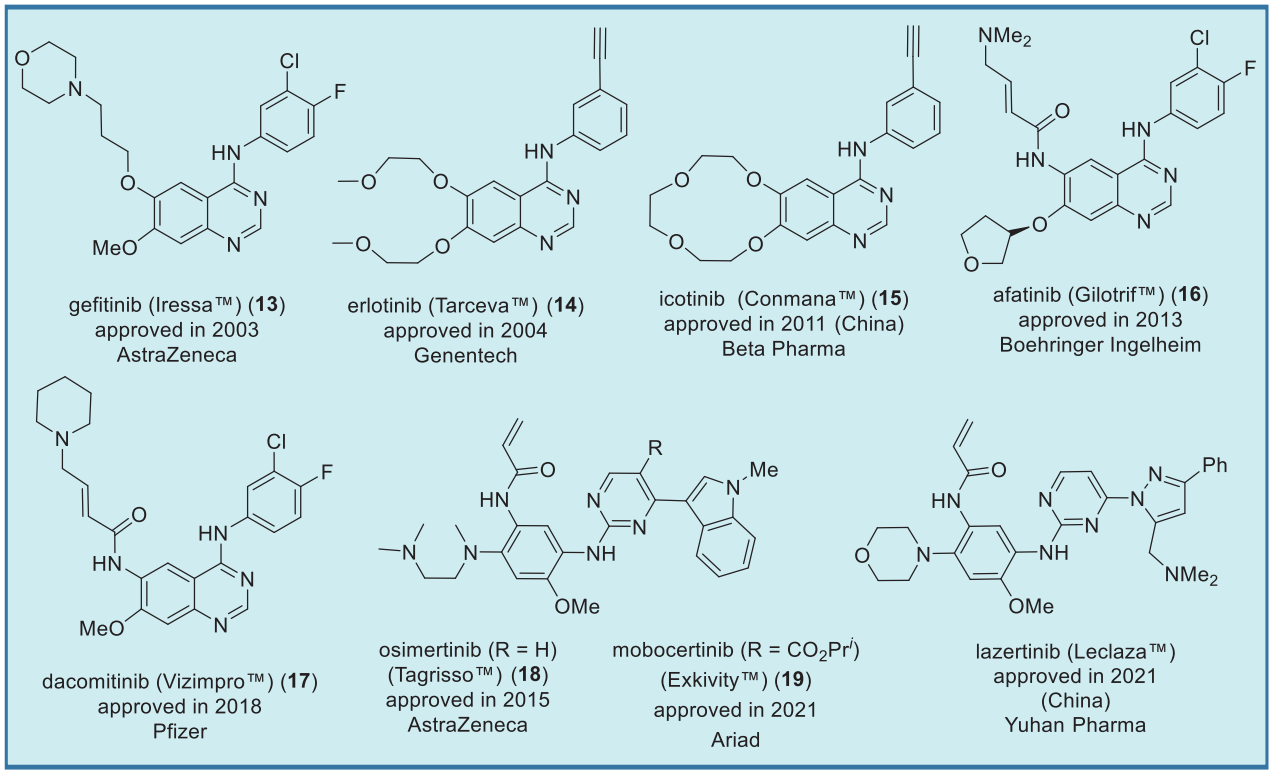

Figure 17. EGFR inhibitors for NSCLC (Chapter 4).

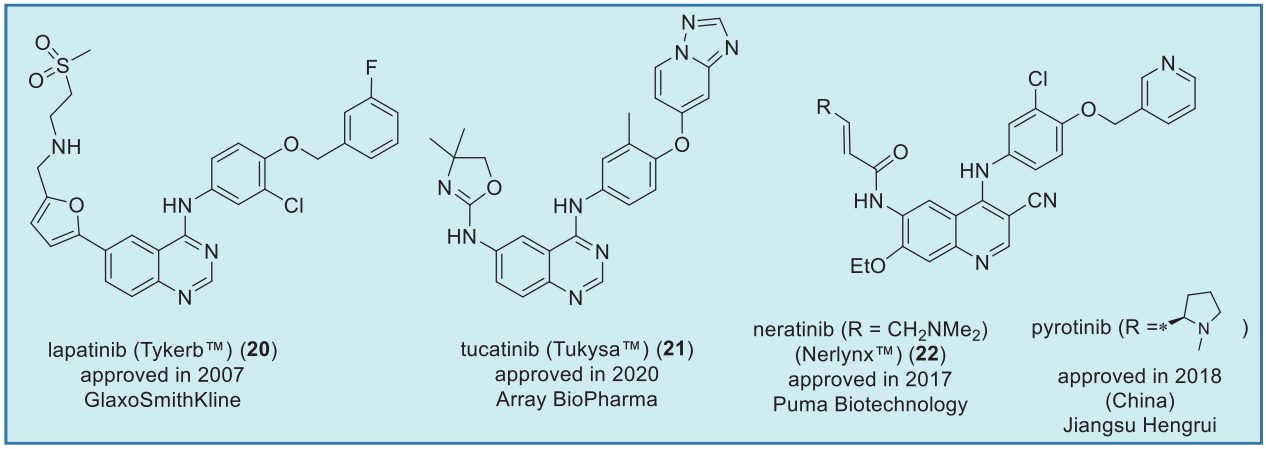

Figure 18. HER2/EGFR inhibitors for HER2+ breast cancer (Chapter 4).

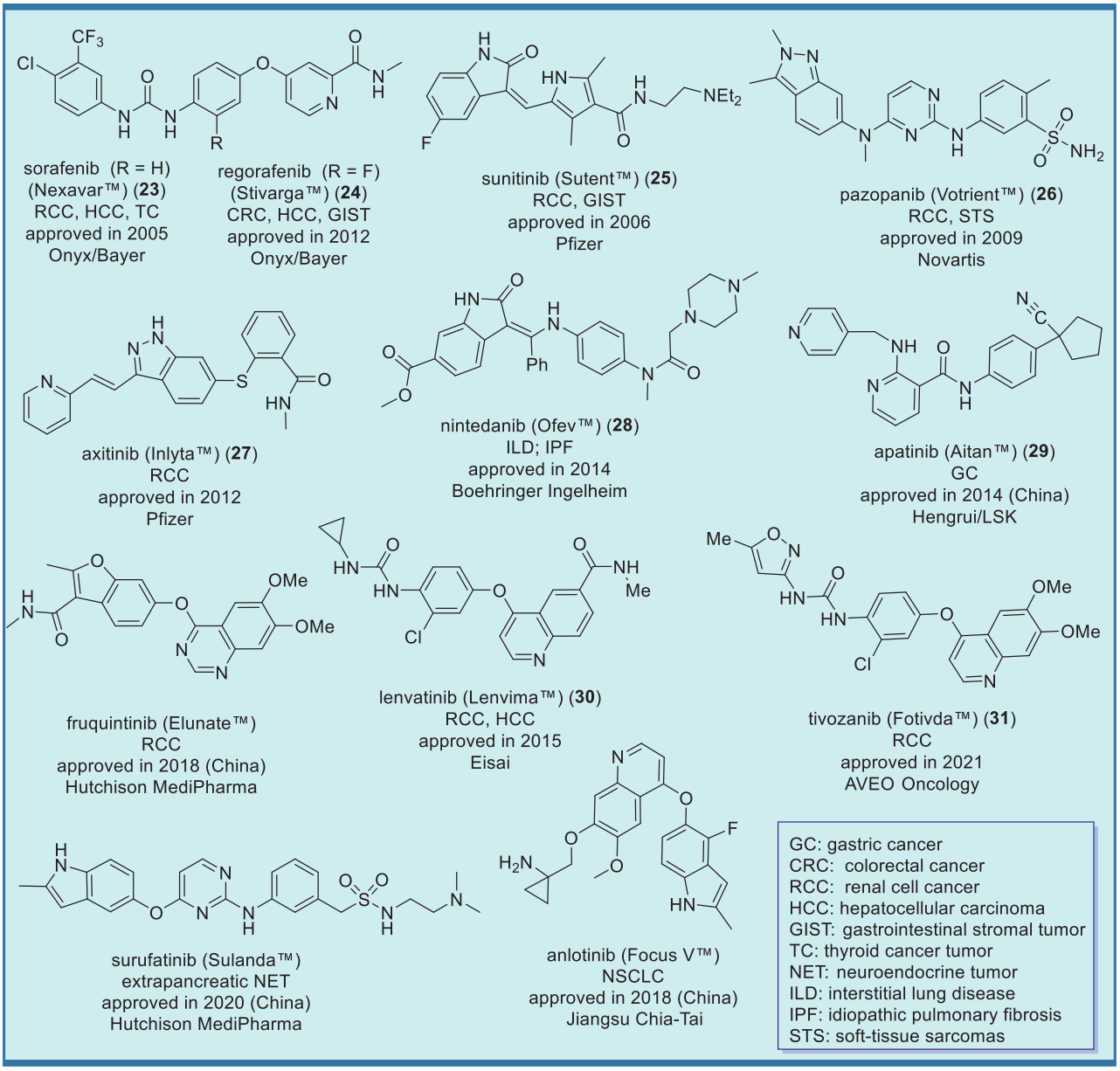

Figure 19. VEGFR/multikinase inhibitors (Chapter 5).

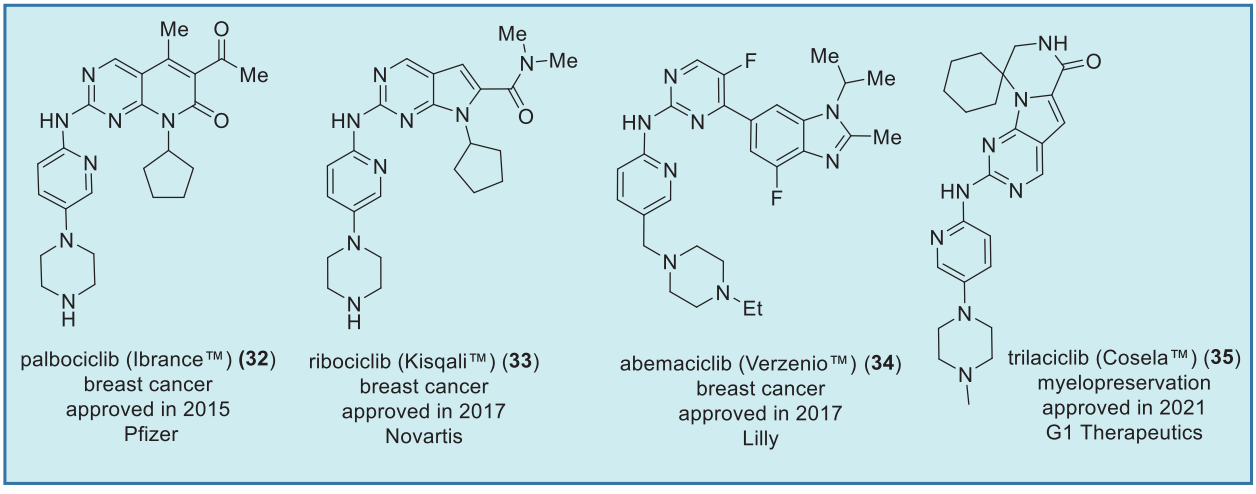

Figure 20. CDK4/6 inhibitors (Chapter 6).

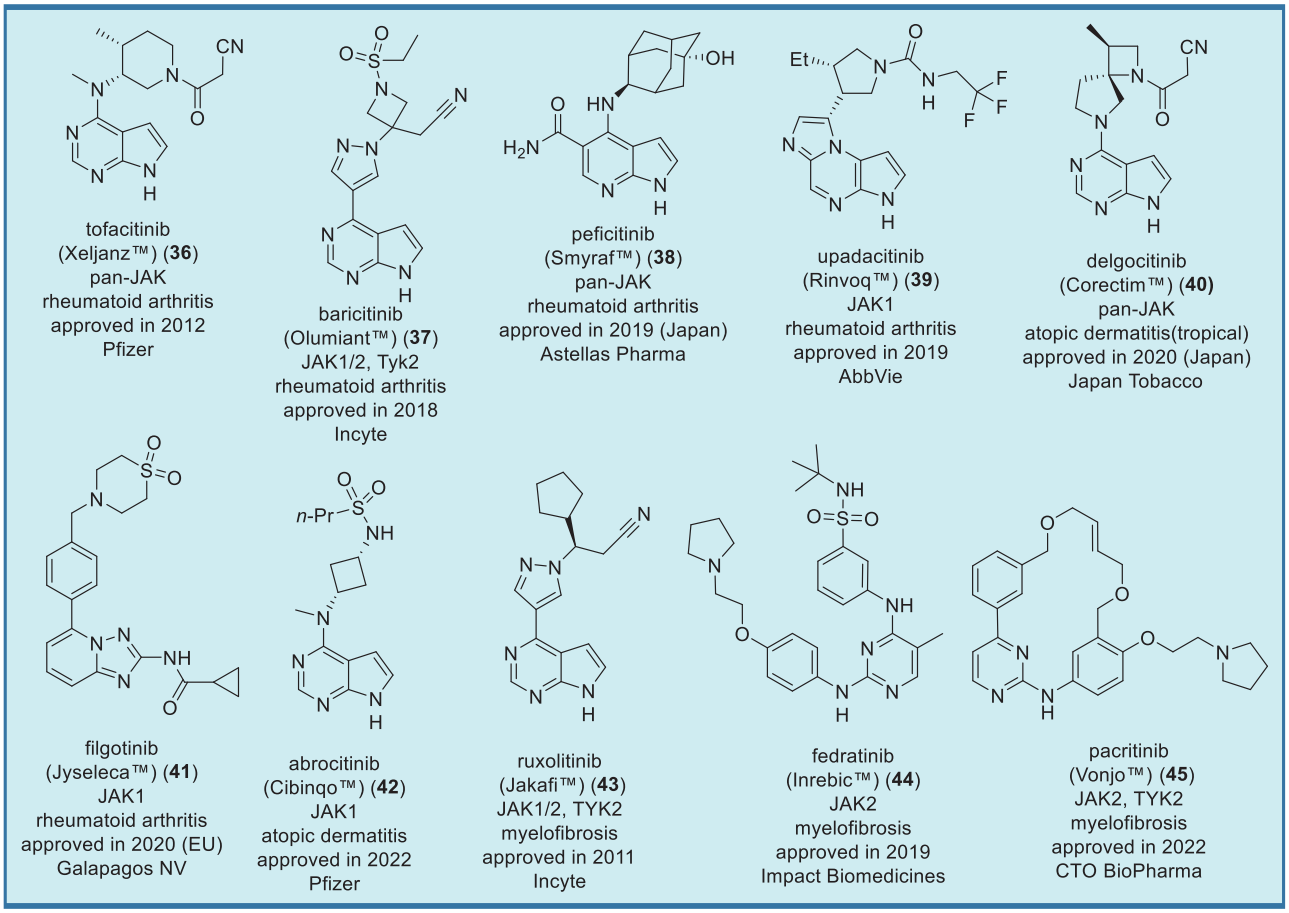

Figure 21. JAK inhibitors (Chapter 7).

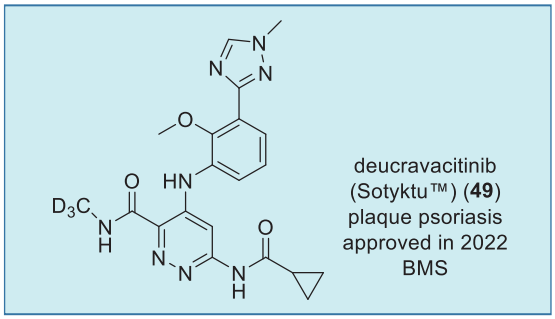

Figure 22. Allosteric TYK2 inhibitor (Chapter 8).

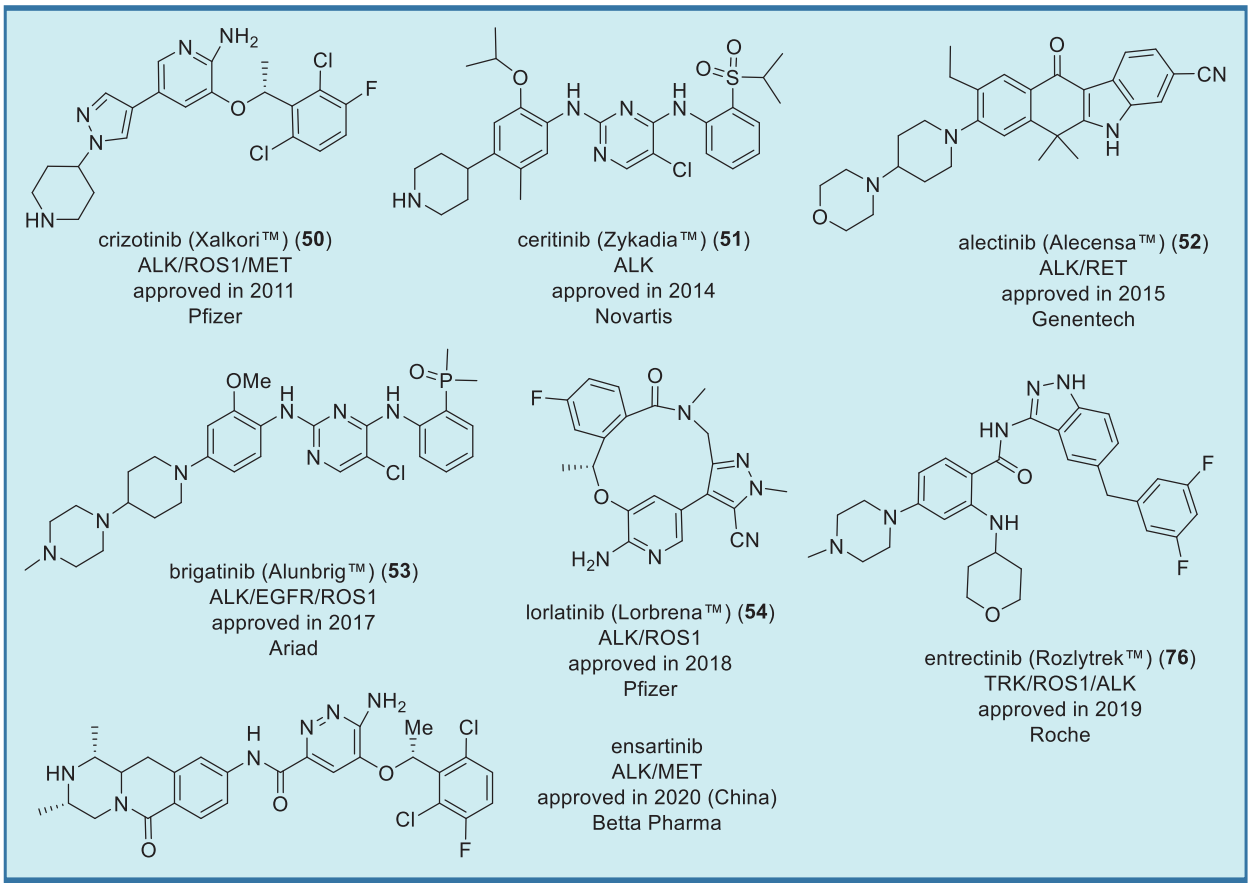

Figure 23. ALK/multikinase inhibitors for NSCLC (Chapter 9).

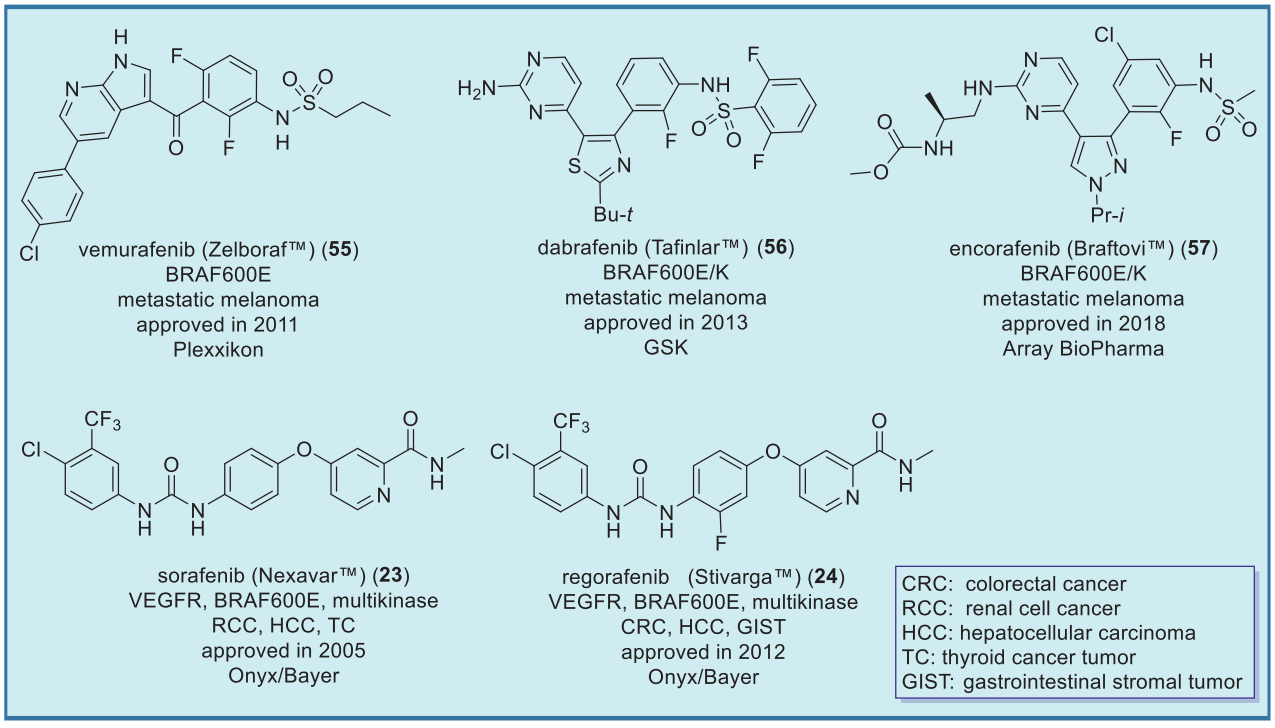

Figure 24. BRAF inhibitors for various cancers (Chapter 10).

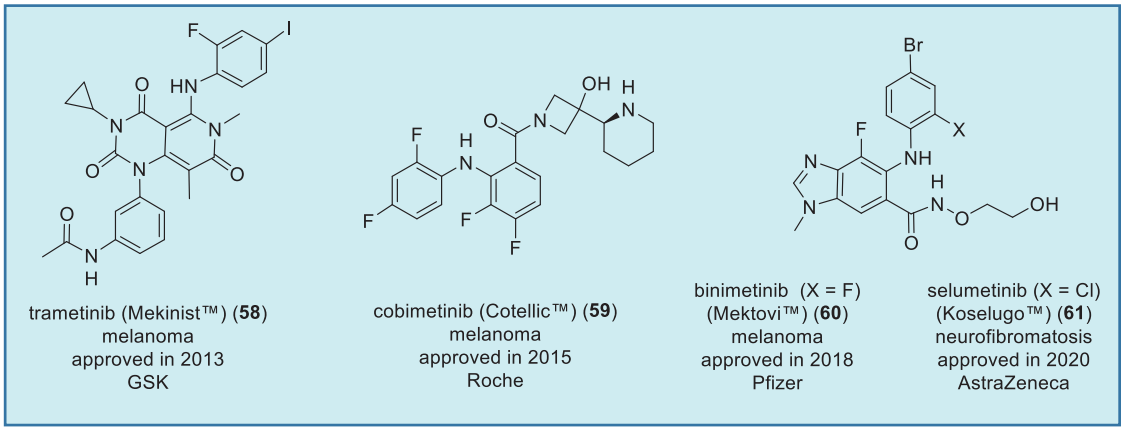

Figure 25. MEK inhibitors (Chapter 11).

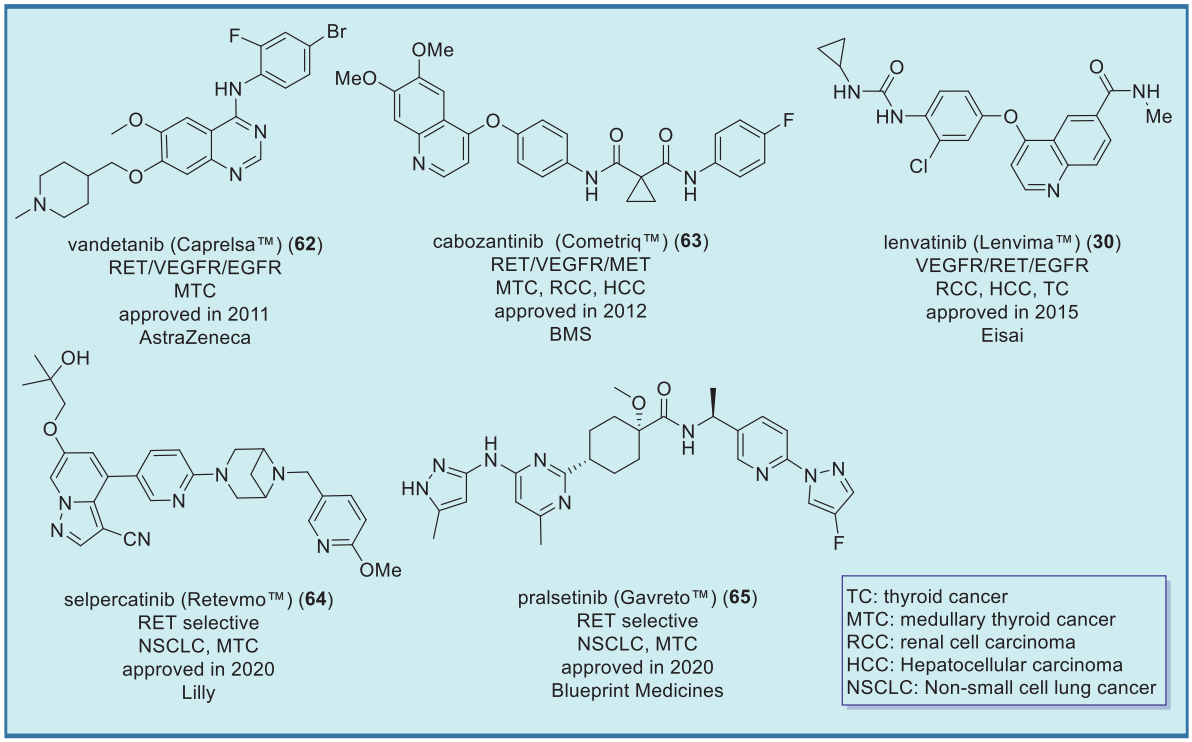

Figure 26. RET/multikinase inhibitors (Chapter 12).

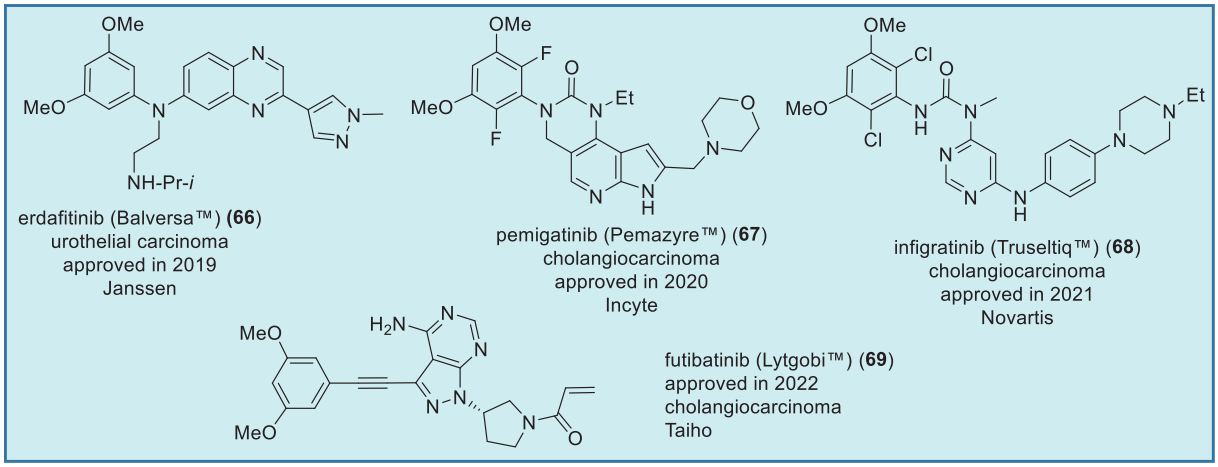

Figure 27. Pan-FGFR inhibitors (Chapter 13).

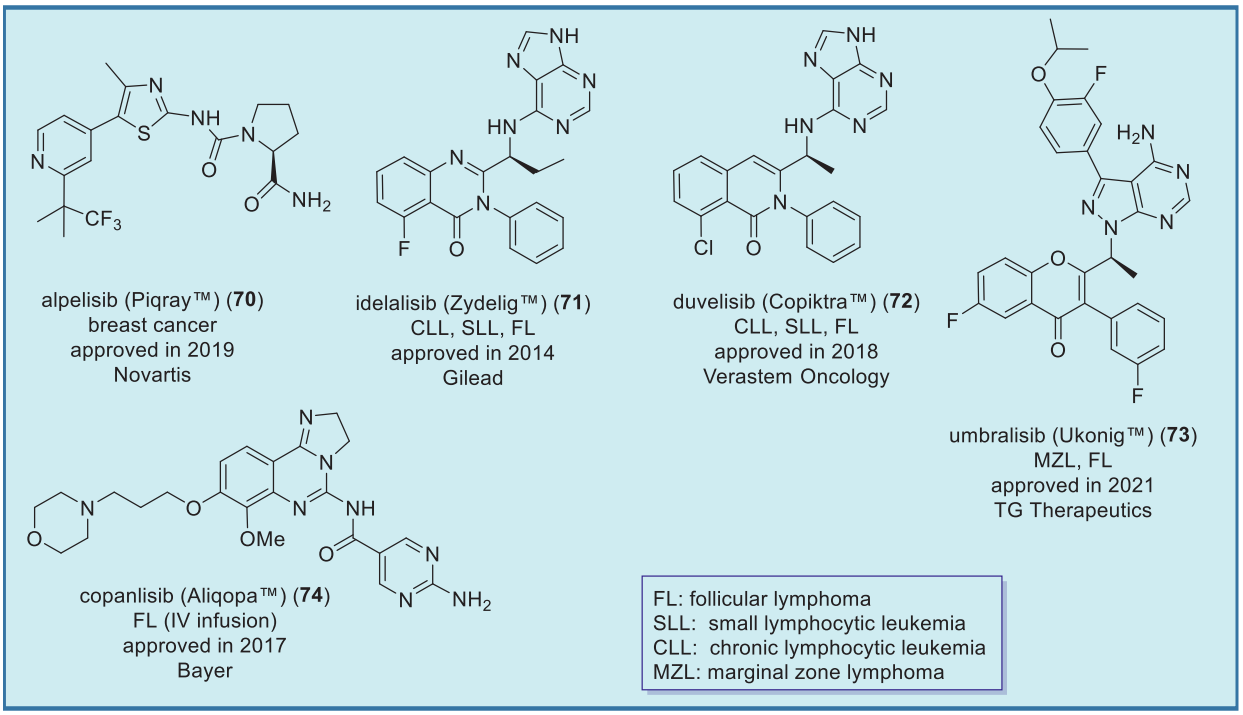

Figure 28. PI3K inhibitors (Chapter 14).

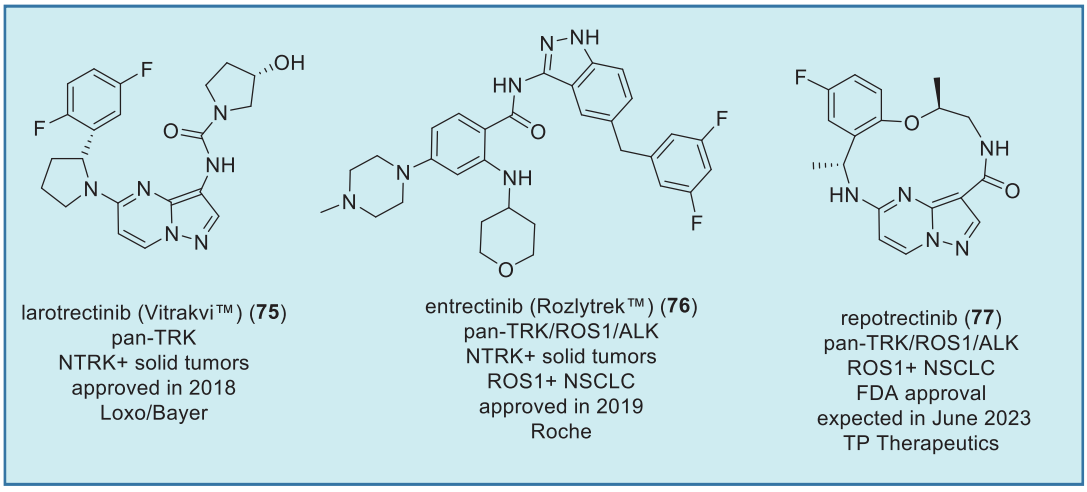

Figure 29. Pan-TRK/multikinase inhibitors (Chapter 15).

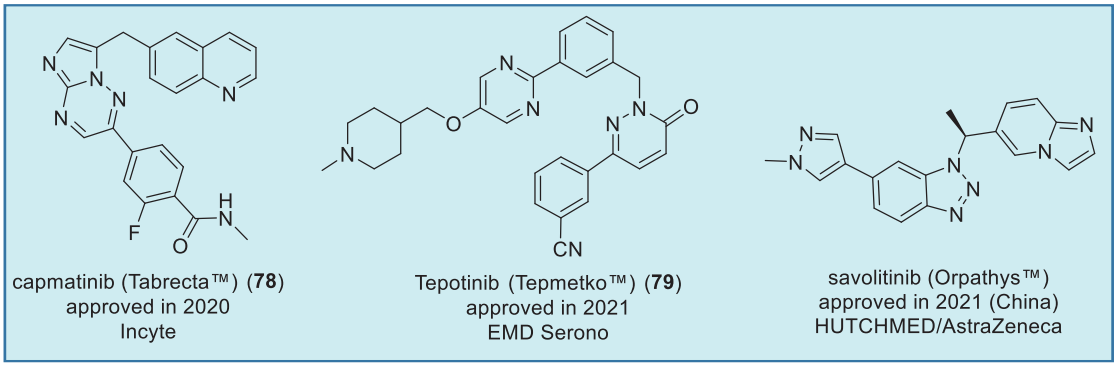

Figure 30. MET inhibitors for MET-altered NSCLC (Chapter 16).

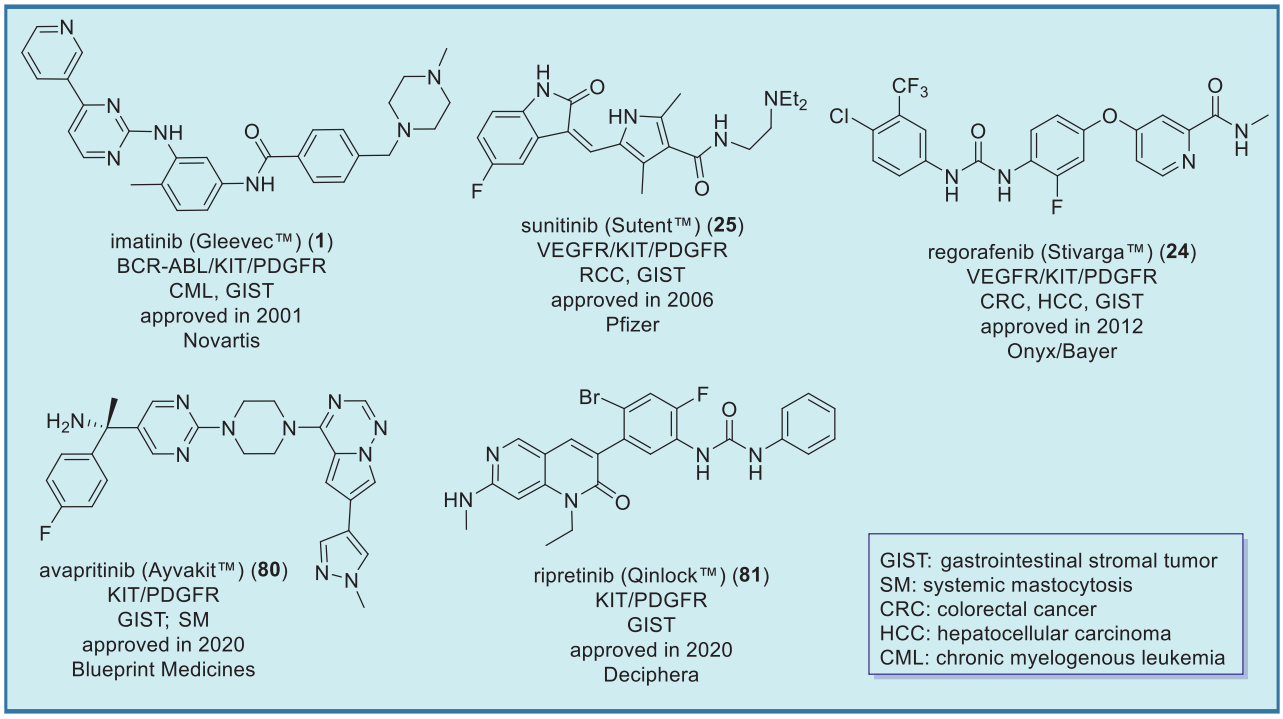

Figure 31. KIT/PDGFR/multikinase inhibitors (Chapter 17).

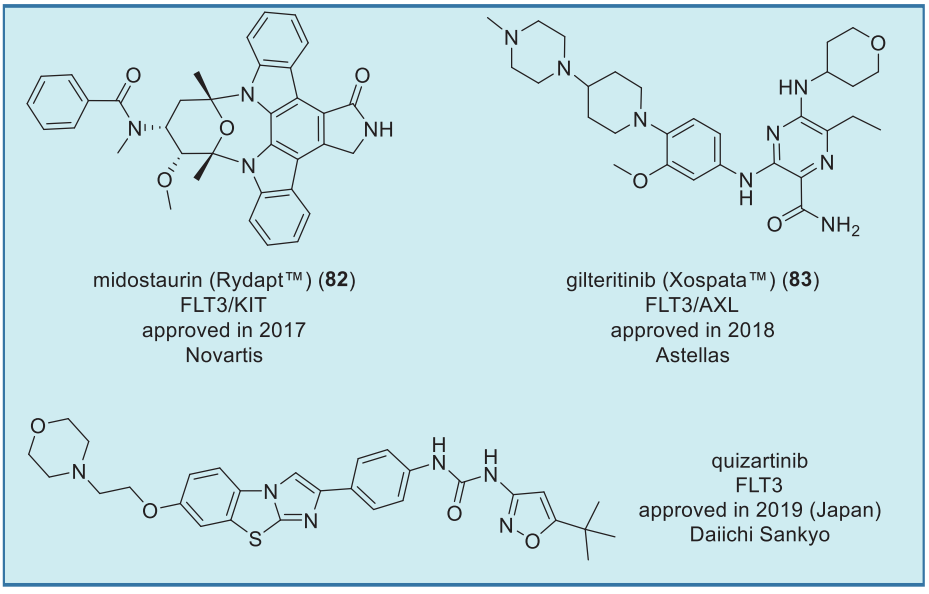

Figure 32. FLT3 inhibitors for FLT3+ AML (Chapter 18).

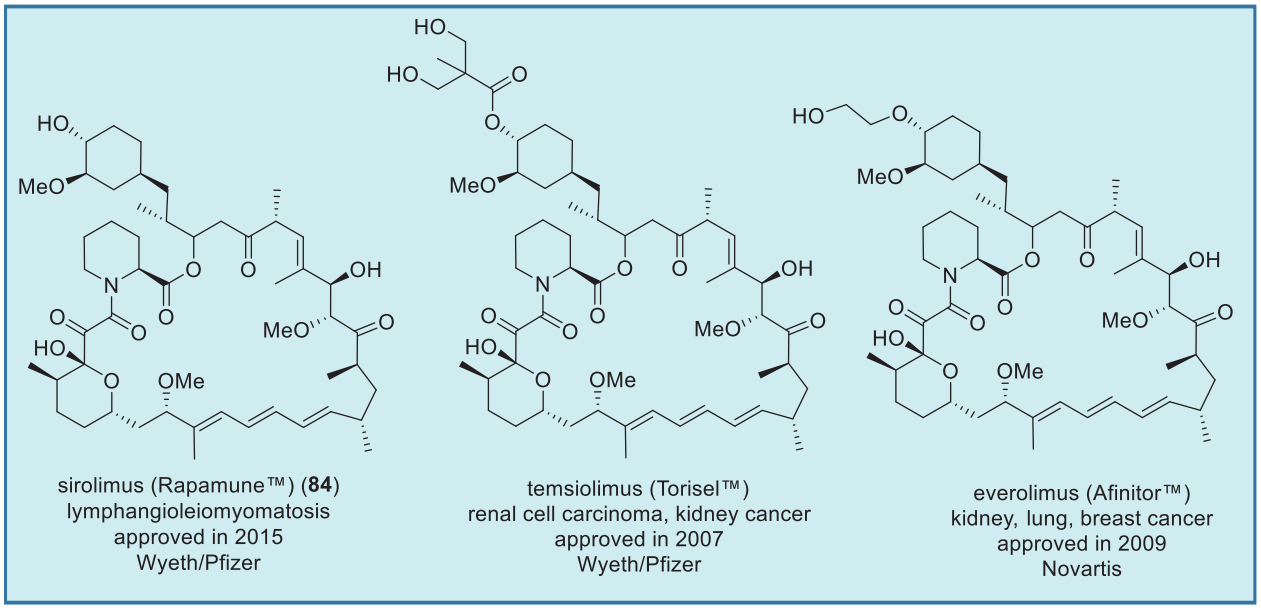

Figure 33. mTOR inhibitors (Chapter 19).

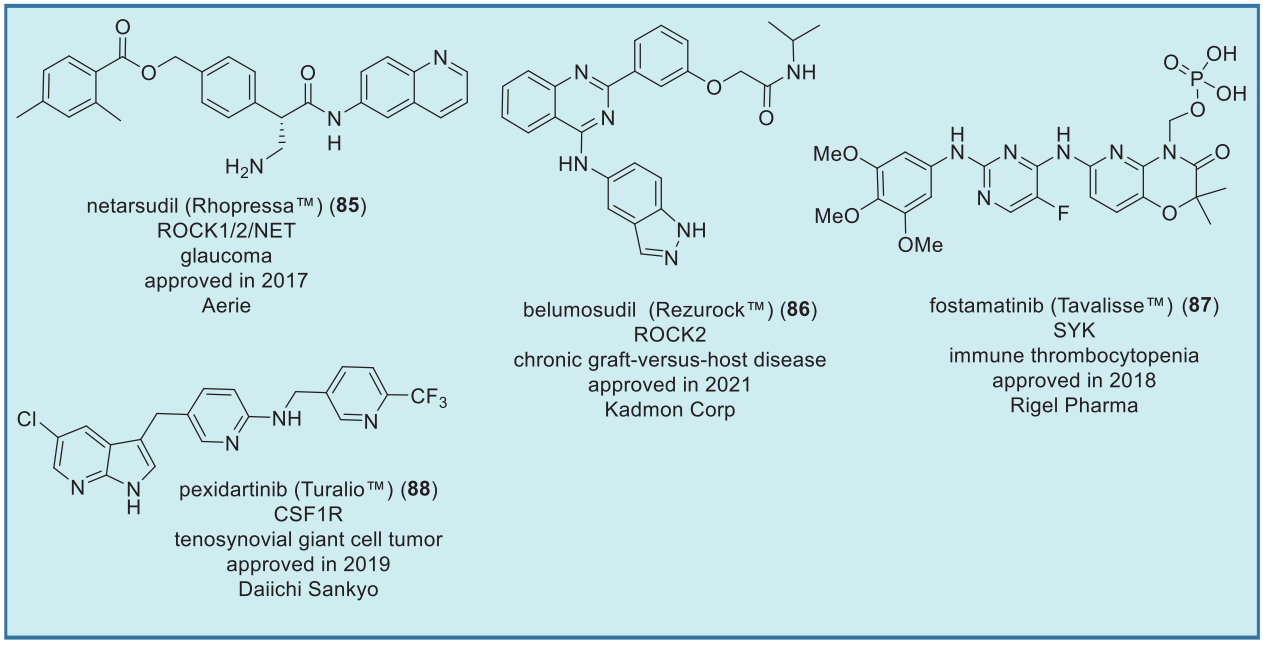

Figure 34. Other kinase inhibitors (Chapter 20).

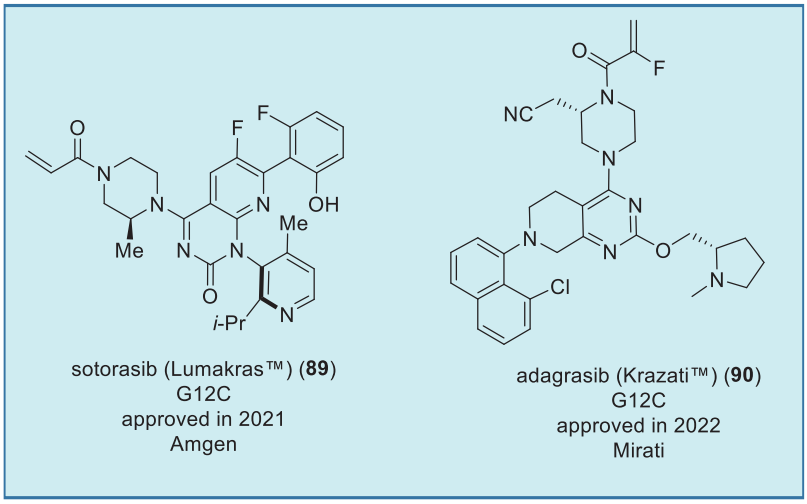

Figure 35. KRASG12C inhibitors (Chapter 21).

1. L. A. Smyth, I. Collins. Measuring and interpreting the selectivity of protein kinase inhibitors. *J. Chem. Biol.* **2009**, *2*, 131–151.
2. T. O'Hare, R. Pollock, E. P. Stoffregen, J. A. Keats Wang B, Wu H, Hu C, Wang H, Liu J, Wang W, Liu Q. An overview of kinase downregulators and recent advances in discovery approaches. *Signal Transduct. Target Ther*. **2021**, *6*, 423.
3. S. R. Hubbard, J. H. Till. Protein tyrosine kinase structure and function. *Annu. Rev. Biochem.* **2000**, *69*, 373–398.
4. S. Kothiwale, C. M. Borza, E. W. Lowe, A. Pozzi, J. Meiler. Discoidin domain receptor 1 (DDR1) kinase as target for structure-based drug discovery. *Drug Discov.Today*. **2015**, 20, 255–261.
5. A. K. Ghose, T. Herbertz, D. A. Pippin, J. M. Salvino, J. P. Mallamo. Knowledge based prediction of ligand binding modes and rational inhibitor design for kinase drug discovery. *J. Med. Chem*. **2008**, *51*, 5149–5171.
6. R. Urich, G. Wishart, M. Kiczun, A. Richters, N. Tidten-Luksch, D. Rauh, B. Sherborne, P. G. Wyatt, R. Brenk. De novo design of protein kinase inhibitors by in silico identification of hinge region-binding fragments. *ACS Chem. Biol.* **2013**, *8*, 1044–1052.
7. P. Mukherjee, J. Bentzien, T. Bosanac, W. Mao, M. Burke, I. Muegge. Kinase crystal miner: A powerful approach to repurposing 3D hinge binding fragments and its application to finding novel bruton tyrosine kinase inhibitors. *J. Chem. Inf. Model*. **2017**, *57*, 2152–2160.
8. G. Scapin. Protein kinase inhibition: Different approaches to selective inhibitor design. *Curr. Drug Targets.* **2006**, *7*, 1443–1454.
9. I. Abdelbaky, H. Tayara, K. T. Chong. Prediction of kinase inhibitors binding modes with machine learning and reduced descriptor sets. *Sci. Rep*. **2021**, *11*, 706.
10. L. K. Gavrin, E. Saiah. Approaches to discover non-ATP site kinase inhibitors. *MedChemComm.* **2013**, *4*, 41–51.
11. P. Y. Lee, Y. Yeoh, T. Y. Low. A recent update on small-molecule kinase inhibitors for targeted cancer therapy and their therapeutic insights from mass spectrometry-based proteomic analysis. *The FEBS J.* **2022**, 10.1111/febs.16442. Advance online publication.
12. R. S. Vijayan, P. He, V. Modi, K. C. Duong-Ly, H. Ma, J. R. Peterson, J. R., Dunbrack, R. M. Levy. Conformational analysis of the DFG-out kinase motif and biochemical profiling of structurally validated type II inhibitors. *J. Med. Chem.* **2015**, *58*, 466–479.
13. D. Fabbro, S. W. Cowan-Jacob, H. Moebitz H. Ten things you should know about protein kinases: IUPHAR Review 14. *Br. J. Pharmacol*. **2015**, *172*, 2675-700.
14. D. E. Heppner, M. J. Eck. A structural perspective on targeting the RTK/Ras/MAP kinase pathway in cancer. *Protein Sci.* **2021**, *30*, 1535–1553.
15. K. Aertgeerts, R. Skene, J. Yano, B. C. Sang, H. Zou, G. Snell, A. Jennings, K. Iwamoto, N. Habuka, A. Hirokawa, T. Ishikawa, T., Tanaka, H. Miki, Y. Ohta, S. Sogabe. Structural analysis of the mechanism of inhibition and allosteric activation of the kinase domain of HER2 protein. *J. Biol. Chem.* **2011**, *286*, 18756–18765.
16. P. Wu, T. E. Nielsen, M. H. Clausen. FDA-approved small-molecule kinase inhibitors. *Trends Pharmacol. Sci.* **2015**, *36*, 422–439.